HHS Public Access

Author manuscript

J Neurosci Methods. Author manuscript; available in PMC 2017 July 15.

Published in final edited form as:

J Neurosci Methods. 2016 July 15; 267: 14–20. doi:10.1016/j.jneumeth.2016.04.004.

Second spatial derivative analysis of cortical surface potentials recorded in cat primary auditory cortex using thin film surface arrays: comparisons with multi-unit data

James B. Fallon[a,b,c], **Sam Irving**[a], **Satinderpall S. Pannu**[d], **Angela C. Tooker**[d], **Andrew K. Wise**[a,b,c], **Robert K. Shepherd**[a,c], and **Dexter R. F. Irvine**[a]

[a] Bionics Institute, Melbourne, Victoria, Australia.

[b] Department of Otolaryngology, University of Melbourne, Melbourne, Victoria, Australia.

[c] Medical Bionics Department, University of Melbourne, Melbourne, Victoria, Australia.

[d] Lawrence Livermore National Laboratory, Livermore, CA.

Abstract

Background—Current source density analysis of recordings from penetrating electrode arrays has traditionally been used to examine the layer-specific cortical activation and plastic changes associated with changed afferent input. We report on a related analysis, the second spatial derivative (SSD) of surface local field potentials (LFPs) recorded using custom designed thin-film polyimide substrate arrays.

Results—SSD analysis of tone-evoked LFPs generated from the auditory cortex under the recording array demonstrated a stereotypical single local minimum, often flanked by maxima on both the caudal and rostral sides. In contrast, tone-pips at frequencies not represented in the region under the array, but known (on the basis of normal tonotopic organization) to be represented caudal to the recording array, had a more complex pattern of many sources and sinks.

Comparison with Existing Methods—Compared to traditional analysis of LFPs, SSD analysis produced a tonotopic map that was more similar to that obtained with multi-unit recordings in a normal-hearing animal. Additionally, the statistically significant decrease in the number of acoustically responsive cortical locations in partially deafened cats following 6 months of cochlear implant use compared to unstimulated cases observed with multi-unit data ($p = 0.04$) was also observed with SSD analysis ($p = 0.02$), but was not apparent using traditional analysis of LFPs ($p = 0.6$).

Conclusions—SSD analysis of surface LFPs from the thin-film array provides a rapid and robust method for examining the spatial distribution of cortical activity with improved spatial resolution compared to more traditional LFP recordings.

Corresponding Author Dr. James Fallon, Bionics Institute, 384-388 Albert Street, East Melbourne, Victoria, Australia, 3002, Ph: +61 3 9667 7576, Fax: +61 3 9667 7518, ; Email: jfallon@bionicsinstitute.org

Keywords

Local field potential; cochlear implant; cortical plasticity; neural prosthesis; sensorineural hearing loss

1. Introduction

Current source density (CSD) analysis has been applied to a wide range of neocortical and other brain structures for over 50 years (Mitzdorf, 1985), and was first used to analyse recordings from auditory cortex by Müller-Preuss & Mitzdorf (1984). More recently, CSD analysis has been used in a number of studies investigating the plastic changes that occur in the auditory cortex as a result of long-term profound deafness and/or chronic intracochlear electrical stimulation (Klinke et al., 1999; Kral et al., 2005; Middlebrooks, 2008; Schroeder et al., 2001).

By taking the second spatial derivative (SSD) of a series of local field potentials (LFPs) generated by the superposition of synaptic events (Cottaris & Elfar, 2009), CSD analysis allows identification of the laminar sources of currents, based on a characteristic pattern of current sources and sinks. CSD analysis of cortical activity presumes the LFPs are dominated by signals from within a single cortical column (Mitzdorf, 1985), and changes that occur in parameters encoded across multiple cortical columns, such as tonotopic organization, consequently cannot be investigated with CSD. However, surface LFPs are well suited to studying these phenomena. They were used in the first demonstrations of the tonotopic organization of primary auditory cortex (AI) (Woolsey & Walzl, 1942), and have been used to investigate the propagation of ‘travelling’ waves of activity across the cortex (Kral et al., 2009). Such studies have typically utilized sequential recordings from small (1 mm in diameter) silver or platinum-ball macroelectrodes, although they can also utilize microelectrode recordings from the cortical surface (e.g.Kral et al., 2009) or the middle cortical layers (e.g.Norena & Eggermont, 2002). The need to average responses to multiple presentations of the same stimuli to extract the small (10 – 100 μV) LFP from background activity, and to move the electrode to successive recording sites, makes these experiments extremely time-consuming. When recordings are made with macroelectrodes, the size of the LFP can also be influenced by the variable contact of the electrode with the cortical surface over the duration of the recordings. A final issue with standard LFP recording is that LFPs are a mixture of locally generated potentials and potentials volume conducted from sites up to 1 cm away (Eggermont et al., 2011; Gaucher et al., 2012; Kajikawa & Schroeder, 2011; Norena & Eggermont, 2002).

The present study describes a method for simultaneous recording of LFPs from a large number of surface recording sites, and a method of analyzing those potentials derived from CSD analysis. The method utilizes a custom designed thin-film polyimide substrate electrode array that was developed to be flexible enough to follow the undulating surface of the primary auditory cortex (AI) in the cat, and allow simultaneous recordings at 32 sites. Analysis of the data by taking the SSD of the LFPs across the major caudal-rostral tonotopic axis of the cat AI effectively ‘sharpens’ the LFP recordings to allow a more detailed analysis

of the underlying activity. These procedures were validated by comparing the tonotopic organization of AI as determined by standard LFP analysis and SSD analysis to that obtained with multi-unit (MU) recordings in a normal-hearing cat. Additionally, the responsiveness of the cortex in two groups of partially deafened cats was assessed, revealing a difference in the acoustic responsiveness of AI in cats that had received chronic intracochlear electrical stimulation compared to partially deafened, unstimulated controls. This difference, which was evident in the MU data and was also in accord with previously reported MU data (Fallon et al., 2009b), was not evident using the standard simpler analysis of the LFPs.

2. Materials and Methods

2.1. Recording Electrode Arrays

Details of the fabrication of these types of arrays have been reported previously (Tooker et al., 2012), and will only be summarized here. The electrode arrays were fabricated using multiple layers of polyimide and metal. The fabrication process began by depositing the first layer of polyimide. A first layer of trace metal (gold) was deposited and patterned, followed by a second layer of polyimide. Interconnection vias were etched into this second layer of polyimide using oxygen plasma. A second layer of trace metal (gold) was then deposited and patterned. The electrode metal (platinum) was next deposited and patterned. A final layer of polyimide was deposited and openings for the electrodes were etched using oxygen plasma.

The novel array geometry described in this study was specifically designed to follow the undulating surface of AI in the cat by utilizing 8 separate fingers, each with 4 electrodes, for a total of 32 electrodes. The electrodes were 200μm in diameter, with 800μm center-to-center spacing. The resulting array allowed coverage of the majority of the surface accessible portion of the cat AI (Figure 2A). Surface tension attracted the array to the cortical surface and the flexible fingers follow the contours of the cortex ensuring all electrodes made good electrical contact with the cortical surface.

2.2. Experimental subjects

Fourteen healthy adult cats with otoscopically normal tympanic membranes and normal hearing were used in the present study. Hearing status was determined using auditory brainstem response (ABR) recordings using standard procedures (Irving et al., 2014), with normal hearing defined as a click-ABR threshold < 32 dB peak equivalent sound pressure level (SPL). All procedures were in accordance with Australian Code of Practice for the Care and Use of Animals for Scientific Purposes and with the Guidelines laid down by the National Institutes of Health in the US regarding the care and use of animals for experimental procedures, and were approved by the Royal Victorian Eye and Ear Hospital Animal Research and Ethics Committee.

2.3. Deafening procedure

Thirteen cats were administered a daily subcutaneous (s.c.) injection of kanamycin sulfate (200 mg/kg) for 17 days (Irving et al., 2014), which preferentially damages the high-

frequency basal region of the cochlea. Tone-evoked ABRs were used to determine the degree of hearing loss achieved. Additional daily kanamycin injections were continued until a satisfactory high-frequency hearing loss (>60 dB HL at frequencies >8 kHz) had been achieved. Mean ABR audiograms for the two partially deafened groups, along with data for a large sample (n = 40 ears) of normal-hearing cats, are shown in Figure 1. Thresholds are similar to normal for frequencies below 2 kHz, but increase progressively up to 10 kHz, and at higher frequencies are at or above our maximum intensity of 100 dB SPL

2.4. Cochlear implantation and chronic stimulation

Approximately six months following deafening, eight partially deafened animals were randomly selected and unilaterally implanted in the left cochlea with a Cochlear Ltd Hybrid L14 cat electrode array (Shepherd et al., 2011), an extra-cochlear ball electrode in the temporalis muscle, and lead-wire assembly, using previously published techniques (Coco et al., 2007). Briefly, surgery was performed under aseptic conditions, with each animal premedicated using atropine/acepromazine (ANAMAV, 0.05 ml/kg s.c.) and maintained at a surgical level of anesthesia using a closed circuit anesthetic machine delivering a mixture of isoflurane (1-3%) and oxygen. The array was inserted to approximately 50% the length of the cat scala tympani, representing a tip electrode position of around 4 kHz (Irving et al., 2014).

Fourteen days after surgery, and every month thereafter during the chronic stimulation program, the cats were anesthetized with ketamine and xylazine (20 mg/kg i.m., 2 mg/kg s.c.) and an electrically evoked ABR (EABR) was recorded for each stimulating electrode. EABR-recording methods were as described previously (Fallon et al., 2009a). Approximately two weeks after the first EABR recordings the chronic stimulation program was initiated. Each animal received continuous unilateral stimulation at all available intra-cochlear electrodes from a Nucleus Freedom speech processor via a clinical stimulator (Cochlear Ltd, Sydney, Australia) situated within a custom-made backpack that was worn by the animal (Fallon et al., 2009a). The speech processors were programmed using standard clinical frequency allocation tables and delivered monopolar stimulation at 500 pulses per second (pps) per electrode. Each biphasic current pulse had a 25-μs phase interval and an 8-μs inter-phase gap, and stimulus level was varied from 3 dB below to 6 dB above the EABR threshold for that electrode. These adult-deaf stimulated (ADS group) cats were chronically stimulated for periods up to 8 months, with stimulation continuing until the commencement of the acute electrophysiological experiments. The acute experiments on the five adult-deafened unstimulated (ADU group) cats were carried out ~6months after deafening.

2.5. Cortical recording

Acute electrophysiological experiments to record surface LFPs from auditory cortex were performed at 38 – 93 weeks of age (see Table 1). Anesthesia was induced with ketamine and xylazine (20 mg/kg i.m., 2 mg/kg s.c.) and maintained at a steady, light level of surgical anesthesia via a slow intravenous infusion of sodium pentobarbitone (0.3 - 0.7 mg/kg/h). A tracheal cannula was inserted and respiration rate, end-tidal CO2, and core body temperature were maintained within normal levels (5-25 breaths/minute, 3-7% and 36-38 °C

respectively). The ADU animals were acutely implanted (left ear) using the same surgical techniques and the same electrode arrays as used for the ADS animals.

Animals were placed in a stereotaxic frame in an electrically shielded room, and a craniotomy was performed to expose the right auditory cortex. The thin-film surface array was placed over the middle ectosylvian gyrus (MEG), extending caudally from the anterior ectosylvian sulcus and ventrally from a position approximately 1 mm ventral of the suprasylvian sulcus (Figure 2A). Surface LFPs were captured at a sample rate of 10 kHz using the Cerebus system (Cyberkinetics; Foxborough, Massachusetts) and processed off-line in IgorPro (Wavemetrics; Lake Oswego, Oregon). Following LFP recordings, MU responses were recorded using standard techniques (Fallon et al., 2009b). Briefly, a 7×7 planar silicon array (Cyberkinetics; Foxborough, Massachusetts) was inserted in the middle of the MEG, and a linear array (A1×32-6mm-100-413-A32, NeuroNexus Technologies; Ann Arbor, Michigan) inserted down the rostral bank of the posterior ectosylvian sulcus. Recordings were captured at a sample rate of 30 kHz using the Cerebus system. At the end of the experiment the animals were terminated with an overdose of sodium pentobarbital (150 mg/kg, intravenous).

2.6. Acoustic stimulation and data analysis

Acoustic stimuli were delivered via a calibrated 4” Vifa XT25TG30–04 speaker (Vifa, Videbæk, Denmark) driven by a TDT SA1 Stereo Power Amp (Tucker Davis Technologies, FL, USA). Stimuli consisted of 100-ms pure-tones (5-ms linear rise/fall) presented at 1 Hz at a range of frequency-intensity combinations (0.5 – 30 kHz in 1 kHz steps; 0 – 100 dB SPL in 5 dB steps). Each stimulus was presented 10 times with stimulus order randomized between repetitions.

For each recording site, the response area (RA) was determined by calculating the peak-to-peak amplitude of the LFP in the 100-ms window following the stimulus onset for each frequency-intensity combination (Figure 2B). These peak-to-peak values were then normalized to the maximum response to any stimulus for that recording site, and used to determine the threshold (the lowest sound pressure level at which the peak-to-peak amplitude was significantly (more than 2 standard deviations) above the background noise level) and characteristic frequency (CF, frequency with the lowest threshold) for that recording site (Figure 2C). In this way the tonotopic organisation for the area under the entire recording array could be determined (Figure 2D).

Additionally, a new analysis based on the second spatial derivative was used to determine the tonotopic organisation. The 32-channel rectangular array was analysed as four separate 8-channel caudal-rostral linear electrode arrays (Figure 3A). For each frequency-intensity combination, the SSD was computed at each sampled time-point from 0 to 100ms post stimulus onset (Figure 3B) according to the formula:

$$SSD_t^d = \frac{\varnothing_t^{r-\Delta r} - 2 \times \varnothing_t^r + \varnothing_t^{r+\Delta r}}{\Delta r^2}$$

where $\varnothing_t^r$ represents the potential amplitudes recorded at caudal-rostral location r with latency t.

For a supra-threshold stimulus, the SSD analysis produced a stereotypical pattern of a single negative maximum (e.g., red area in Figure 3C) flanked in the caudal and rostral directions by positive maxima (e.g., dark blue areas at 20ms in Figure 3C). For each frequency – intensity combination, the location along the caudal-rostral axis at which the largest negative maximum occurred was used in plots of frequency against caudal-rostral position (Figure 3E) to determine the tonotopic organization.

Finally, MU activity was analyzed using standard techniques (Fallon et al., 2009a). Briefly, MU RAs were determined from the number of threshold (set to −4 times the root-mean-squared background) crossings in the 5 – 55 ms following stimulus onset. These spike counts were then normalized to the maximum response to any stimulus for that recording site, and used to determine the threshold (normalised response significantly above the background level) and CF.

3. Results

Tone-evoked LFPs could be recorded from all fourteen animals. The LFPs from the normal-hearing animal (6-19) will be used to demonstrate several features of the SSD analysis, and provide an initial validation of this analysis by comparison with MU data. Additional validation will be provided by a comparison of LFP, SSD and MU data from the ADS and ADU animals concerning the effects of partial deafness and cochlear electrical stimulation on acoustic responsiveness.

As illustrated in Figure 2C, the CF for a given recording site is defined as the frequency with the lowest threshold; therefore, the tonotopic organisation observed using CF (Figure 2D) is defined only at threshold levels. At supra-threshold stimulus levels the best frequency (BF; the frequency eliciting the largest response at a particular sound pressure level) is sometimes used, and as is clear from Figure 2C, the BF can change with stimulation level (the maximum response shifts to lower frequencies with increasing level in Figure 2C and is 11kHz at 70 dB SPL). In contrast, with SSD analysis of the LFPs the location of the central negative maximum is relatively insensitive to level, provided the stimulus is supra-threshold (Figure 3D). The overlap of the different symbols, representing different stimulus intensities, in Figure 3E highlights this level invariance of the central negative maximum for a given stimulus frequency. The location of the central negative maximum does, however, shift with stimulus frequency (Figure 3E and Figure 4B, Pearson correlation; $P < 0.001$) and exhibits the expected caudal-rostral shift with increasing stimulus frequency). Plots of CF against caudo-rostral position for the LFP and MU data are shown Figure 4A and C respectively, and the linear fits for three analyses are plotted together in Figure 4D. The slope of the SSD function (5.5 kHz / mm) is similar to that computed from the MU CFs (4.9 kHz / mm), and both are substantially higher than that computed from the LFP CFs (3.8 kHz / mm), consistent with the finding that CF gradients determined from LFPs underestimate the true gradient (Eggermont et al., 2011).

In Figure 5, the proportions of recording sites to which frequencies could be assigned using LFP, SSD and MU analyses are shown for the normal-hearing cat and the two groups of partially deafened cats. For the normal-hearing cat, the proportions are similar (in the range 80-90%) for the three methods. In the LFP analysis, the proportion of locations to which a CF could be assigned was reduced by approximately 20% in the partially deafened cats, to 69.3% ± 9.7% and 62.1% ± 9.1% (mean ± standard error of the mean) sites in the ADU and ADS animals, respectively. This difference between the two partially deafened groups was not significant (t-Test, t= 0.5466, p = 0.597). In contrast, the proportion of sites that were assigned a frequency by the SSD analysis was substantially reduced (by 50% or more) in the partially deafened animals: only 33.3% ± 2.9% and 18.8% ± 4.2% mean ± standard error of the mean) of the recording sites in the ADU and ADS groups, respectively, exhibited a local minimum. In contrast to the LFP analysis, this difference between the groups was significant (t-Test, t= 2.824, p = 0.017). Finally, the proportion of locations to which a CF could be assigned with the MU analysis was even further reduced; only 15.9% ± 9.5% and 5.7% ± 6.9% mean ± standard error of the mean) of the recording sites in the ADU and ADS groups, respectively. As with the SSD analysis, this difference was significant (t-Test, t=1.950, p = 0.0399). Both the SSD and MU analyses therefore differ from the LFP analysis in showing a substantial reduction of responsive sites in the partially deafened animals and a significant difference between the ADU and ADS groups.

4. Discussion

The use of a thin-film polyimide substrate electrode array to record surface LFPs provides several advantages over sequential recordings made with either macro- or micro-electrodes. The greatest advantage is the ability to record simultaneously from large cortical regions, which eliminates possible confounds with changes in cortical responsiveness over time. The reduction in recording time is a further advantage, as it potentially allows more data to be obtained within a given experiment. The ability of the flexible electrode array, combined with the specific geometry of the fingers of electrodes, to conform to surface topology, also results in more consistent recording conditions. Furthermore, simultaneous recording from multiple sites allows the use of SSD analysis of the surface LFPs. Finally, the less invasive nature of the surface electrode, compared to MU recording electrodes, would be expected to results in improved long-term performance during chronic implantation.

The tonotopic organization of the primary auditory cortex on the cat's MEG was originally established using LFP recordings (Woolsey & Walzl, 1942) and has been described in detail using MU recordings (Aitkin, 1990; Merzenich et al., 1975; Reale & Imig, 1980). The frequency-to-cortex mapping using MU recordings in the normal-hearing cat in the current study was 4.9 kHz / mm, within the range of 5.3 ± 0.3 kHz / mm we have previously reported using MU recordings from penetrating microelectrodes in normal-hearing cats (Fallon et al., 2009a). The value of 5.5 kHz / mm obtained with SSD analysis also falls within this normal MU data range. In contrast, the mapping using LFP analysis was 3.0 kHz / mm. This shallower mapping is consistent with the broader spreading of LFPs resulting in underestimation of the gradient as determined with spiking activity (Eggermont et al., 2011). The effective increase in the spatial resolution obtained with SSD analysis of

the LFPs brings it within the range achievable with more invasive single-unit or MU recording, and constitutes a significant advantage of this technique.

The improved spatial resolution of the SSD analysis also allowed us to observe a significant reduction in the proportion of acoustically responsive sites in the MEG of partially deafened cats following chronic intra-cochlear stimulation. This finding is consistent with our previous report using standard electrophysiology and penetrating microelectrodes in neonatally ototoxically partially deafened animals (Fallon et al., 2009b). The proportions in our previous study (82% and 58% for unstimulated and stimulated groups respectively) are much higher than those in the present study, reflecting the fact that recordings in that study were made with single microelectrodes. The ability to move the electrode throughout the depth of the cortex in the search for driven activity greatly increases the possibility of being able to determine a CF. The important point, however, is that the SSD analysis revealed a difference that has been seen consistently in MU activity but was not apparent using the standard CF analysis of the LFPs. As noted above, volume conduction spatially smears the LFPs, and this smearing is ameliorated by the improved spatial resolution provided by the SSD analysis.

The data we have presented establish that the SSD analysis provides descriptions of normal AI tonotopy, and of responsiveness in partially deafened animals, that are much more similar to those provided by MU data than are descriptions based on LFP analysis. A feature not captured by the SSD analysis is the change in BF that can occur with stimulation level with both MU and LFP analysis (see Figure 2C). In fact, SSD analysis is relatively insensitive to level, provided the stimulus is supra-threshold (see Figure 3D). The reasons for this level-invariance of assigned frequency with the SSD method are unclear, but would not seem to offset its advantages unless the issue under consideration were the effects of level on frequency selectivity.

The current thin-film polyimide substrate electrode array has been specifically designed for AI in the cat, although it could be easily adapted to other cortical areas (e.g. primary visual cortex) or other species. Design modifications for different sized cortical areas would need to trade-off the number of electrodes and the center-to-center spacing. The current design utilizes 800 μm center-to-center spacing as the LFP signal drops by ~50% in 400 μm (Cottaris & Elfar, 2009), but the spacing could be adjusted as required. As the exposed electrode materials of platinum and polyimide are biological compatible, the use of the thin-film polyimide substrate electrode array and SSD analysis could provide a viable method of chronically monitoring cortical plasticity in humans, without the injury concerns of using penetrating electrode arrays (Jorfi et al., 2015). Finally, the SSD analysis may prove useful in the analysis of other surface recordings such as epilepsy monitoring and brain machine interfaces.

Acknowledgments

This work was funded by the NH&MRC (GNT1002430) and National Institute of Deafness and Other Communication Disorders (NIH Y1-DC-8002-01) and Lawrence Livermore National Laboratory. The Bionics Institute acknowledges the support it receives from the Victorian Government through its Operational Infrastructure Support Program.

We thank Vanessa Tolosa, Kedar Shah, Sarah Felix and Nicole Critch for technical assistance.

Abbreviations

ABR	Auditory brainstem response
AI	Primary auditory cortex
ICES	Intra-cochlear electrical stimulation
SEM	Standard error of the mean

References

Aitkin, L. Structural and Functional Bases of Auditory Perception. Chapman and Hall; London, UK: 1990. The Auditory Cortex..

Coco A, Epp SB, Fallon JB, Xu J, Millard RE, Shepherd RK. Does cochlear implantation and electrical stimulation affect residual hair cells and spiral ganglion neurons? Hear Res. 2007; 225:60–70. [PubMed: 17258411]

Cottaris N, Elfar S. Assessing the efficacy of visual prostheses by decoding ms-LFPs: application to retinal implants. J Neural Eng. 2009; 6:026007. [PubMed: 19289859]

Eggermont JJ, Munguia R, Pienkowski M, Shaw G. Comparison of LFP-based and spike-based spectro-temporal receptive fields and cross-correlation in cat primary auditory cortex. PLoS One. 2011; 6:e20046. [PubMed: 21625385]

Fallon JB, Irvine DRF, Shepherd RK. Cochlear implant use following neonatal deafness influences the cochleotopic organization of the primary auditory cortex in cats. J Comp Neurol. 2009a; 512:101–114. [PubMed: 18972570]

Fallon JB, Shepherd RK, Brown M, Irvine DR. Effects of neonatal partial deafness and chronic intracochlear electrical stimulation on auditory and electrical response characteristics in primary auditory cortex. Hear Res. 2009b; 257:93–105. [PubMed: 19703532]

Gaucher Q, Edeline JM, Gourevitch B. How different are the local field potentials and spiking activities? Insights from multi-electrodes arrays. Journal of physiology, Paris. 2012; 106:93–103.

Irving S, Wise AK, Millard RE, Shepherd RK, Fallon JB. A partial hearing animal model for chronic electro-acoustic stimulation. J Neural Eng. 2014; 11:046008. [PubMed: 24921595]

Jorfi M, Skousen JL, Weder C, Capadona JR. Progress towards biocompatible intracortical microelectrodes for neural interfacing applications. J Neural Eng. 2015; 12:011001. [PubMed: 25460808]

Kajikawa Y, Schroeder CE. How local is the local field potential? Neuron. 2011; 72:847–58. [PubMed: 22153379]

Klinke R, Kral A, Heid S, Tillein J, Hartmann R. Recruitment of the auditory cortex in congenitally deaf cats by long-term cochlear electrostimulation. Science. 1999; 285:1729–33. [PubMed: 10481008]

Kral A, Tillein J, Heid S, Hartmann R, Klinke R. Postnatal cortical development in congenital auditory deprivation. Cereb Cortex. 2005; 15:552–62. [PubMed: 15319310]

Kral A, Tillein J, Hubka P, Schiemann D, Heid S, Hartmann R, Engel AK. Spatiotemporal patterns of cortical activity with bilateral cochlear implants in congenital deafness. J Neurosci. 2009; 29:811–27. [PubMed: 19158306]

Merzenich MM, Knight PL, Roth GL. Representation of cochlea within primary auditory cortex in the cat. J Neurophysiol. 1975; 38:231–49. [PubMed: 1092814]

Middlebrooks JC. Auditory cortex phase locking to amplitude-modulated cochlear implant pulse trains. J Neurophysiol. 2008; 100:76–91. [PubMed: 18367697]

Mitzdorf U. Current source-density method and application in cat cerebral cortex: investigation of evoked potentials and EEG phenomena. Physiological Reviews. 1985; 65:37–100. [PubMed: 3880898]

Müller-Preuss P, Mitzdorf U. Functional anatomy of the inferior colliculus and the auditory cortex: current source density analyses of click-evoked potentials. Hear Res. 1984; 16:133–142. [PubMed: 6526745]

Norena A, Eggermont JJ. Comparison between local field potentials and unit cluster activity in primary auditory cortex and anterior auditory field in the cat. Hear Res. 2002; 166:202–13. [PubMed: 12062772]

Reale RA, Imig TJ. Tonotopic organization in auditory cortex of the cat. J Comp Neurol. 1980; 192:265–91. [PubMed: 7400399]

Schroeder CE, Lindsley RW, Specht C, Marcovici A, Smiley JF, Javitt DC. Somatosensory input to auditory association cortex in the macaque monkey. J Neurophysiol. 2001; 85:1322–1327. [PubMed: 11248001]

Shepherd R, Verhoeven K, Xu J, Risi F, Fallon J, Wise A. An improved cochlear implant electrode array for use in experimental studies. Hear Res. 2011; 277:20–27. [PubMed: 21540098]

Tooker, A.; Tolosa, V.; Shah, KG.; Sheth, H.; Felix, S.; Delima, T.; Pannu, S. Optimization of multi-layer metal neural probe design, Engineering in Medicine and Biology Society (EMBC). 2012 Annual International Conference of the IEEE; IEEE; 2012. p. 5995-5998.

Woolsey CN, Walzl EM. Topical projection of nerve fibers from local regions of the cochlea to the cerebral cortex. Bulletin of Johns Hopkins Hospital. 1942; 71:315–344.

Highlights

A conformable 2-dimension thin-file electrode array is described.

A method for improved spatial resolution of local field potentials is described.

Results obtained with the new method are in agreement with multi-unit data

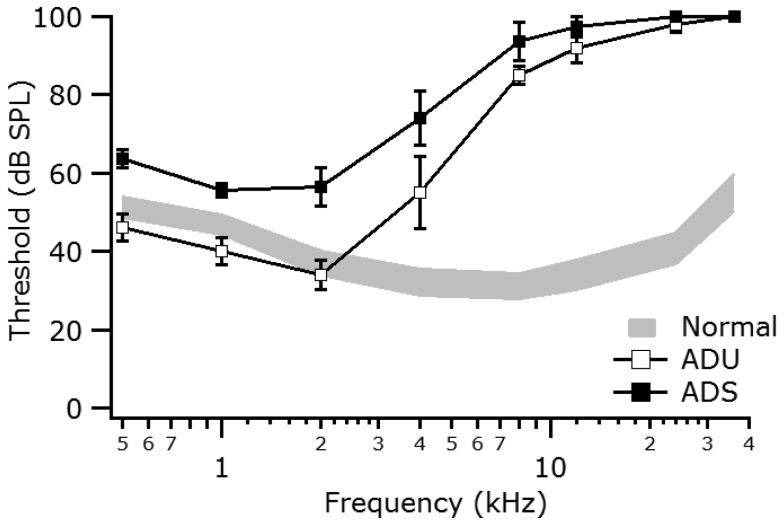

Figure 1.

Auditory brainstem response audiograms for the adult partially deafened unstimulated (ADU) and adult deafened stimulated (ADS) animals at the time of the acute electrophysiological experiment. Values are mean (± standard error of the mean). Grey area indicates the 95% confidence range for normal-hearing animals (n=40 ears).

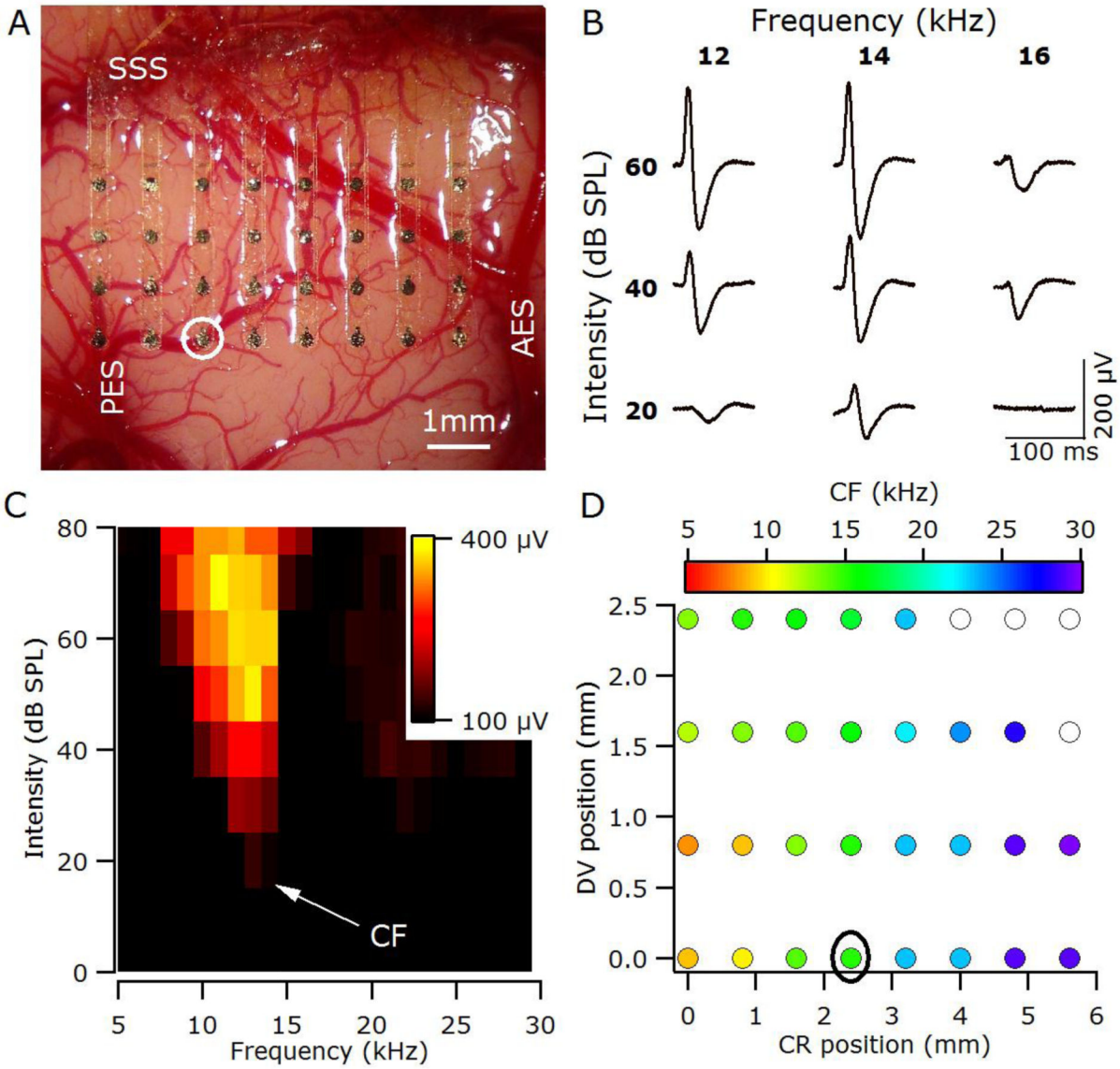

Figure 2.

(A) The thin-film recording array covers the majority of the right primary auditory cortex in a normal-hearing animal (6_19). SSS, suprasylvian sulcus; AES, anterior ectosylvian sulcus; PES, posterior ectosylvian sulcus. (B) Sample local field potentials (LFPs) recorded from the location circled in A & D. LFPs are the averaged response to 10 stimuli, with the first 100 ms of the response shown. (C) Response area, plots the peak-to-peak amplitude of the LFP (yellow-maximum, black minimum) for the recording site circled in A & D. The CF for this site was 14 kHz. (D) Tonotopic organisation of auditory cortex determined using analysis of response areas based on LFPs. Filled symbols represent the characteristic frequency (CF) at each recording site. Open symbols indicate recordings sites for which it was not possible to determine a CF; CR, caudal-rostral position relative to electrode closest to the tip of PES; DV, dorsalventral position relative to electrode closest to the tip of PES.

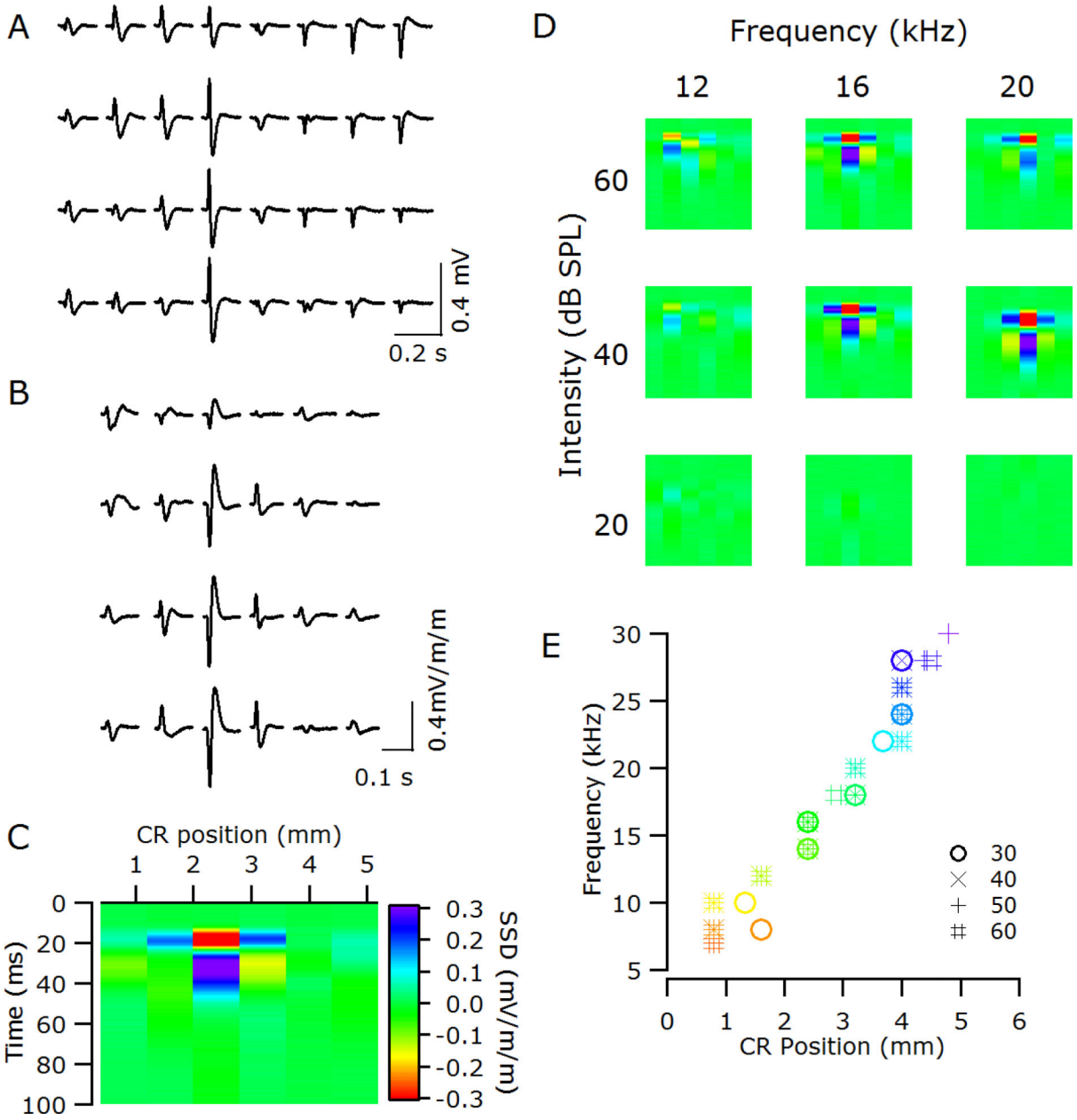

Figure 3.

(A) Sample local field potentials (LFPs) recorded to a 60 dB SPL 16 kHz tone across the thin-film array in a normal-hearing animal (6_19). (B) The second spatial derivative (SSD) of the LFPs evoked by that stimulus. (C) The bottom row of the array exhibits a single negative maximum at 2.4 mm rostral of the tip of the posterior ectosylvian sulcus, which is flanked in the caudal and rostral directions by positive maxima. The positioning of the SSD is relative to the responses illustrated in A & B. (D) Sample SSDs from the bottom row of the array in response to different frequency-intensity combinations (same conventions as C). (E) Tonotopic organization of auditory cortex in 6_19 determined using SSD analysis. Different symbols represent analysis at different dB SPLs; color scale matches Figure 2D.

CR, caudal-rostral position relative to electrode closest to the tip of the posterior ectosylvian sulcus.

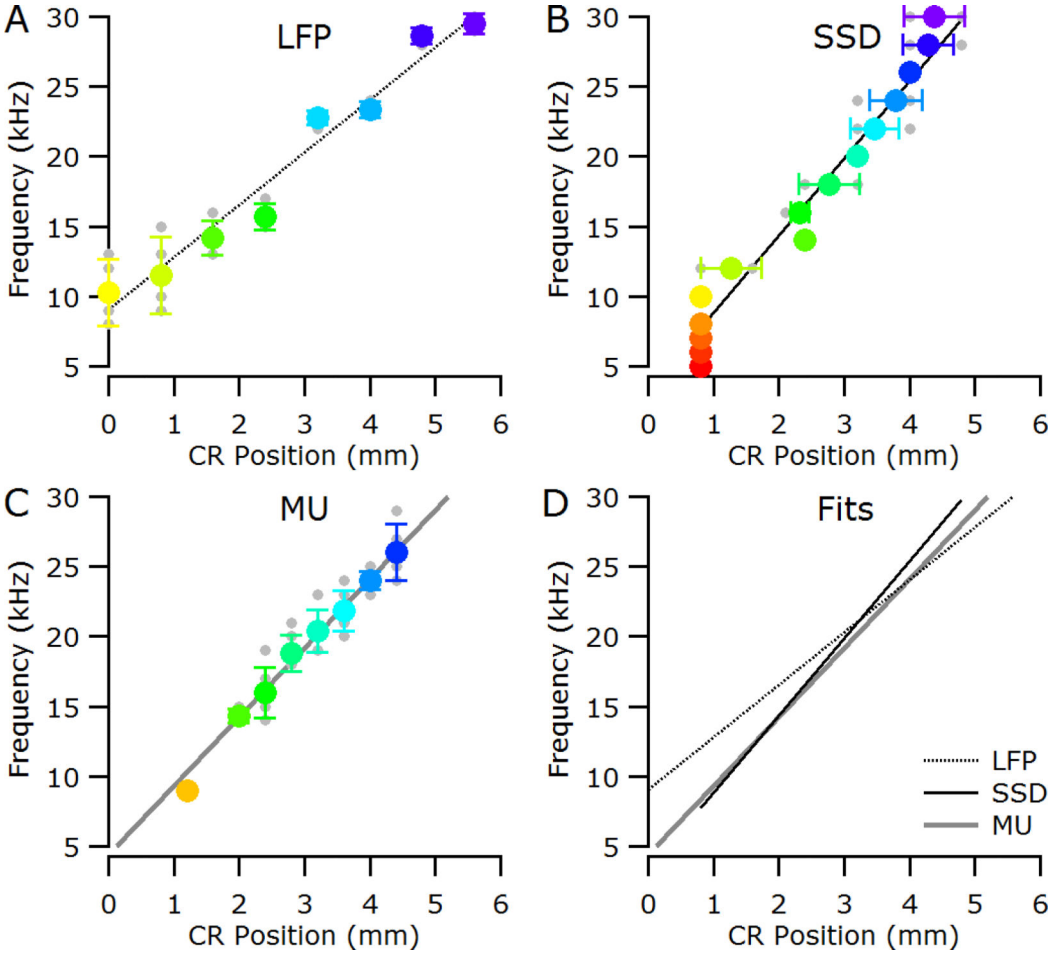

Figure 4.

Data from a normal-hearing cat (6_19). (A) Characteristic frequency (CF) as determined from the LFP response areas plotted against caudal-rostral position. (B) Location of the negative maximum in the SSD analysis for a given stimulus frequency. (C) CF as determined from the multi-unit (MU) activity plotted against caudal-rostral position. In all panels, individual data points are shown in grey; colored symbols are mean (± standard deviation). Lines represent fits to the caudal-rostral shift with increasing stimulus frequency. (D) Overlay of the linear fits for LFP, SSD and MU analysis. CR, caudal-rostral position relative to electrode closest to the tip of the posterior ectosylvian sulcus.

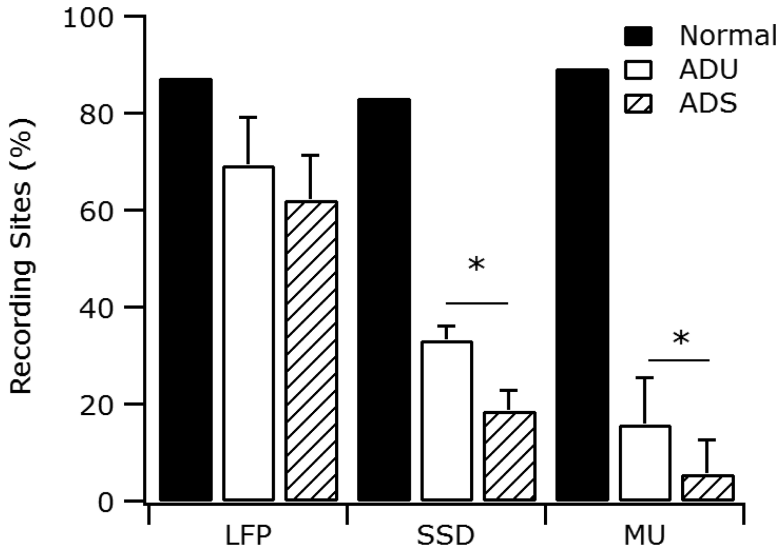

Figure 5.

Proportion of recording sites to which frequencies could be assigned for the three groups of animals using standard local field potential response area analysis (LFP), SSD analysis and multi-unit (MU) activity. There was a significant difference between the adult deafened unstimulated (ADU) and adult deafened stimulated (ADS) groups (*, $p < 0.05$) using the both the SSD and MU analyses but not the standard LFP analysis.

Table 1

Details of deafening and stimulation times for individual animals

Group	Animal ID	Deafening (weeks)	Chronic Stimulation (weeks)	Age (weeks)
Normal-Hearing Control (NHC)	6_19	-	-	38
Adult deafened unstimulated (ADU)	6_23	44	-	73
	6_24	45	-	69
	6_25	35	-	58
	6_27	45	-	74
	6_28	32	-	59
Adult deafened stimulated (ADS)	6_02	31	68	88
	6_11	34	66	93
	6_12	34	66	91
	6_13	34	66	92
	6_14	35	69	91
	6_15	35	70	93
	6_16	35	69	88
	6_17	36	70	88

Individual animals in the experimental groups are specified by identification (ID) number; Deafening is the age at the initiation of deafening injections; Chronic Stimulation is the age at the beginning of the ICES regime which continued until the acute experiment; Age is the age at the time of the acute experiment.